doi:10.1006/jmbi.2001.4648 available online at http://www.idealibrary.com on IDEAL® *J. Mol. Biol.* (2001) **309**, 437–445

JMB

The Lys103Asn Mutation of HIV-1 RT: A Novel Mechanism of Drug Resistance

Yu Hsiou[1], Jianping Ding[1,2], Kalyan Das[1], Arthur D. Clark Jr[1] Paul L. Boyer[3], Paul Lewi[4], Paul A. J. Janssen[4], Jörg-Peter Kleim[5] Manfred Rösner[5], Stephen H. Hughes[3] and Edward Arnold[1]*

[1]*Center for Advanced Biotechnology and Medicine (CABM) and Rutgers University Chemistry Department, 679 Hoes Lane Piscataway, NJ 08854-5638, USA*

[2]*Institute of Biochemistry and Cell Biology, The Chinese Academy of Sciences, 320 Yue-Yang Road, Shanghai 200031, China*

[3]*ABL-Basic Research Program NCI-Frederick Cancer Research and Development Center P.O. Box B, Frederick MD 21702-1201, USA*

[4]*Center for Molecular Design Janssen Research Foundation Antwerpsesteenweg 37 B-2350, Vosselaar, Belgium*

[5]*Hoechst AG, General Pharma Research, G 838 65926 Frankfurt, Germany*

**Corresponding author*

Inhibitors of human immunodeficiency virus (HIV) reverse transcriptase (RT) are widely used in the treatment of HIV infection. Loviride (an α-APA derivative) and HBY 097 (a quinoxaline derivative) are two potent non-nucleoside RT inhibitors (NNRTIs) that have been used in human clinical trials. A major problem for existing anti-retroviral therapy is the emergence of drug-resistant mutants with reduced susceptibility to the inhibitors. Amino acid residue 103 in the p66 subunit of HIV-1 RT is located near a putative entrance to a hydrophobic pocket that binds NNRTIs. Substitution of asparagine for lysine at position 103 of HIV-1 RT is associated with the development of resistance to NNRTIs; this mutation contributes to clinical failure of treatments employing NNRTIs. We have determined the structures of the unliganded form of the Lys103Asn mutant HIV-1 RT and in complexes with loviride and HBY 097. The structures of wild-type and Lys103Asn mutant HIV-1 RT in complexes with NNRTIs are quite similar overall as well as in the vicinity of the bound NNRTIs. Comparison of unliganded wild-type and Lys103Asn mutant HIV-1 RT structures reveals a network of hydrogen bonds in the Lys103Asn mutant that is not present in the wild-type enzyme. Hydrogen bonds in the unliganded Lys103Asn mutant but not in wild-type HIV-1 RT are observed between (1) the side-chains of Asn103 and Tyr188 and (2) well-ordered water molecules in the pocket and nearby pocket residues. The structural differences between unliganded wild-type and Lys103Asn mutant HIV-1 RT may correspond to stabilization of the closed-pocket form of the enzyme, which could interfere with the ability of inhibitors to bind to the enzyme. These results are consistent with kinetic data indicating that NNRTIs bind more slowly to Lys103Asn mutant than to wild-type HIV-1 RT. This novel drug-resistance mechanism explains the broad cross-resistance of Lys103Asn mutant HIV-1 RT to different classes of NNRTIs. Design of NNRTIs that make favorable interactions with the Asn103 side-chain should be relatively effective against the Lys103Asn drug-resistant mutant.

Keywords: AIDS; drug resistance; HIV-1 reverse transcriptase; non-nucleoside inhibitor; X-ray crystallography

Y.H. and J.D. contributed equally to this work.

Present addresses: Paul L. Boyer and Stephen S. Hughes, National Cancer Institute, NCI-Frederick Cancer Research and Development Center, P.O. Box B, Frederick, MD 21702-1201, USA; Jörg-Peter Kleim, Glaxo Wellcome Research and Development, Clinical Virology, Gunnels Wood Road, Stevenage, Hertfordshire, SG1 2NY, UK.

Abbreviations used: HIV-1, human immunodeficiency virus type 1; RT, reverse transcriptase; NNRTIs, non-nucleoside RT inhibitors; NNIBP, non-nucleoside inhibitor binding pocket; AIDS, acquired immunodeficiency syndrome.

E-mail address of the corresponding author: arnold@cabm.rutgers.edu

0022-2836/01/020437–9 $35.00/0

Introduction

Acquired immunodeficiency syndrome (AIDS), a disease of epidemic proportions, is caused by the human immunodeficiency virus (HIV). More than 33 million people are currently infected with HIV, which is a retrovirus. HIV reverse transcriptase (RT) is an essential enzyme that carries out the synthesis of the double-stranded DNA from the single-stranded RNA genome. HIV RT is an asymmetric heterodimer consisting of a p66 subunit and a p51 subunit. Two types of RT inhibitors, nucleoside inhibitors (NRTIs) and non-nucleoside inhibitors (NNRTIs), are among the drugs most widely used for the treatment of AIDS. The efficacy of these highly potent inhibitors is limited by drug-resistant mutants that emerge under drug selection pressure. NRTIs bind to the normal dNTP substrate-binding site and inhibit HIV replication by terminating DNA chain elongation. NNRTIs bind to a hydrophobic pocket in the p66 subunit near the polymerase active site, and inhibit the chemical step of polymerization.

Most NNRTIs select for multiple mutations in or near the NNRTI-binding pocket (NNIBP) of HIV-1 RT in *in vitro* experiments, including Lys103, Tyr181, and Tyr188. The Lys103Asn mutation is selected both *in vitro* and *in vivo* by numerous NNRTIs and is commonly seen in patients receiving NNRTI therapy.[1–7] HIV-1 RT containing the Lys103Asn mutation is ten- to 100-fold resistant to most NNRTIs, including nevirapine, α-APA, BHAP, and TIBO. HBY 097 and loviride (also known as α-APA R90385) are potent NNRTIs that have been tested in human clinical trials.[8–12]

The structure of HIV-1 RT has been studied extensively, providing significant insights into the mechanisms of polymerization, inhibition, and drug-resistance. Among numerous crystal structures of HIV-1 RT are: (1) HIV-1 RT complexed with double-stranded DNA template-primers both in the presence[13] and in the absence of a bound dNTP substrate;[14,15] (2) HIV-1 RT complexed with NNRTIs;[16–26] (3) HIV-1 RT with no bound ligands;[27–29] and (4) HIV-1 RT mutants resistant to NNRTIs[16,"22] and NRTIs.[30,31]

In all the reported structures of RT/NNRTI complexes, the inhibitor binds to HIV-1 RT in a hydrophobic pocket (called the non-nucleoside inhibitor binding pocket or NNIBP) located between the β6-β10-β9 and β12-β13-β14 sheets of the p66 subunit. A small portion of the pocket is formed by residues from the p51 subunit; there is no separate second pocket in p51. No NNIBP exists in unliganded HIV-1 RT structures; its formation requires rearrangement of local structural elements that comprise the pocket. Amino acid residues where mutations confer resistance to NNRTIs, such as Lys103, Tyr181, and Tyr188, are clustered around the binding pocket and are located relatively close to the bound inhibitors. Mutations can affect inhibitor binding by: (1) loss of important contacts between protein and inhibitor; (2) reduction in the size of the binding pocket or modification of pocket shape, and (3) interference with inhibitor entry into the binding pocket. The structures of Tyr181Cys and Tyr188Leu mutant HIV-1 RT in complexes with 8-Cl-TIBO[16] and HBY 097,[22] respectively, have been reported. Both Tyr181 and Tyr188 are located within the NNIBP and have extensive interactions with many NNRTIs. Loss of contacts between the bound inhibitor and mutated amino acid residues appeared to be the primary cause of resistance for these two mutant HIV-1 RTs. In both of those studies, the conformation of the inhibitors was altered in the mutant complexes, apparently to compensate for the loss of interactions caused by the mutation(s).

Lys103 is involved in the formation of the NNIBP. Residue 103 is located at the outer rim of the NNIBP and in the vicinity of an entrance to the pocket.[17] Although there are a number of structures of HIV-1 RT/NNRTI complexes, Lys103 has direct interactions with only one inhibitor, delavirdine (a BHAP derivative). The relatively large delavirdine molecule is only partially contained within the NNIBP; a portion of the inhibitor protrudes from the pocket.[19] Possible effects of Lys103Asn mutation include altering the properties of the NNIBP, and affecting inhibitor entry into the pocket. This could explain the broad spectrum of cross-resistance seen with the NNRTIs. A proposed effect of the Lys103Asn mutation was to introduce a hydrogen bond between Asn103 and Tyr188, a key NNIBP residue.[25] Crystal structures of Lys103Asn mutant HIV-1 RT, both unliganded and with bound NNRTIs, should provide insight into the mechanism of resistance caused by the Lys103Asn mutation.

Results and Discussion

Wild-type and Lys103Asn mutant RT/NNRTI complexes are quite similar

We have determined the structures of the Lys103Asn mutant RT complexed with HBY 097 at 2.8 Å resolution and with loviride at 3.0 Å resolution. Both complexes crystallized with the symmetry of space group *C*2 and the unit cell dimensions were comparable to those of the corresponding wild-type RT/NNRTI complexes. The binding modes of these inhibitors to Lys103Asn RT are quite similar to those seen in the corresponding wild-type RT/NNRTI complexes;[18,22] there are only subtle changes observed in the NNIBP region. This would indicate that, in the bound state, both inhibitors have similar interactions with the Lys103Asn mutant and wild-type HIV-1 RT. Similar observations were reported recently about a complex of Lys103Asn HIV-1 RT with efavirenz.[32]

Mutation from lysine to asparagine reduces the length of the side-chain and changes the overall charge of the binding-pocket region. Clear electron density for the side-chain of Asn103 in the p66 and p51 subunits in both RT/HBY 097 and RT/loviride

complexes indicates that Asn103 is well ordered in both subunits. This differs from the behavior of the Tyr181Cys and Tyr188Leu in their respective drug-resistant mutant RT/NNRTI complex structures;[16,22] in both cases, the mutated residues were disordered in the p66 subunit, but ordered in the p51 subunit. In p66, the Asn side-chain at position 103 is oriented in a direction similar to that seen for Lys103 in both the wild-type RT/loviride and RT/HBY 097 complexes. In p51, the side-chain orientation of Asn103 is slightly different from that of the Lys side-chain in the wild-type structure, possibly due to the change in the size and charge of the amino acid in the mutant protein.

Both inhibitors bind to the mutant RT in the well-defined binding pocket region adjacent to the polymerase active site in the p66 subunit (Figure 1(a) and (b)). Whilst loviride adopts the commonly seen butterfly-like geometry,[17] the binding mode of HBY 097 is similar to that seen in its wild-type complex; this inhibitor does not have a butterfly-like shape in either the wild-type or Lys103Asn mutant RT complex. The overall positions and orientations of both loviride and HBY 097 are quite similar in their complexes with Lys103Asn mutant and wild-type HIV-1 RT. Comparison based on the superposition of all C^{α} positions between the wild-type HIV-1 RT/HBY 097 and Lys103Asn mutant HIV-1 RT/HBY 097 complex shows an RMS deviation of 0.86 Å. Comparing the C^{α} positions in the NNIBP region gives an RMS deviation of 0.57 Å. Two potential hydrogen bonds between HBY 097 and the main-chain atoms of Lys101 (N2-O (Lys101) = 2.9 Å, and S1-N (Lys101) = 3.5 Å) are present in complexes of both wild-type and mutant Lys103Asn RT with HBY 097. The displacements between corresponding HBY 097 atoms in the wild-type and Lys103Asn HIV-1 RT complexes are greatest for the relatively flexible side-groups of the inhibitor, while the

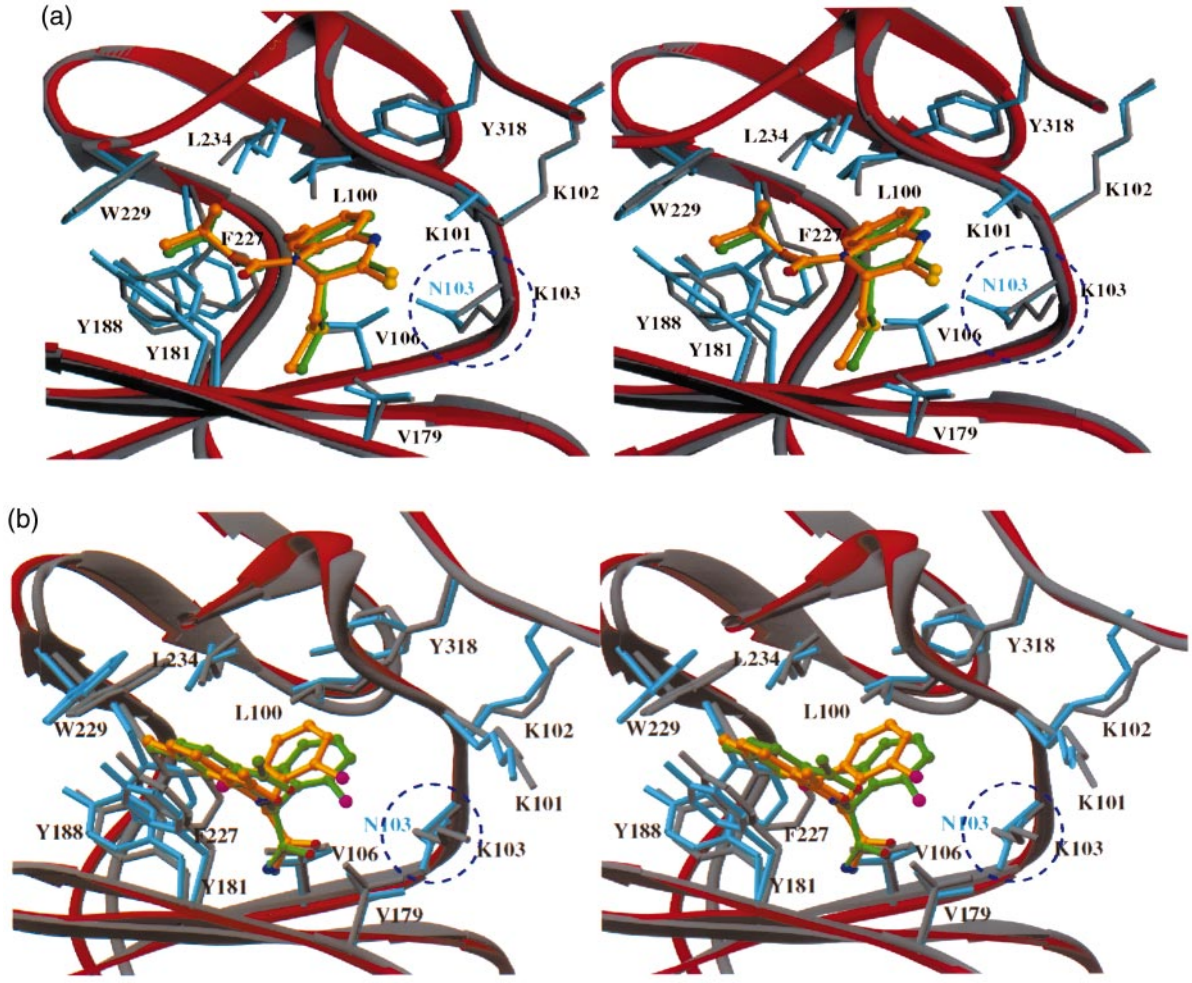

Figure 1. Stereoview of a superposition in the NNIBP region (based on the C^{α} atoms in the p66 palm subdomain) of (a) wild-type HIV-1 RT/HBY 097 and Lys103Asn mutant HIV-1 RT/HBY 097 complexes and (b) wild-type HIV-1 RT/loviride and Lys103Asn mutant HIV-1 RT/loviride complexes, showing the similarities in the binding-pocket region between wild-type and mutant HIV-1 RT. Wild-type HIV-1 RT is shown in gray ribbon, mutant HIV-1 RT in red ribbon with cyan side-chains. The inhibitor complexed with wild-type HIV-1 RT is shown in green, and with mutant HIV-1 RT in gold. The blue circle highlights the position of residue 103.

changes of the orientation and position of the HBY 097 ring system are minimal.

Comparison between the wild-type HIV-1 RT/loviride and the Lys103Asn mutant HIV-1 RT/loviride complex shows an RMS deviation of 0.96 Å for all C^{α} positions and an RMS deviation of 0.50 Å for the C^{α} positions in the NNIBP region. Possible hydrogen-bonding interactions between loviride and the main-chain atom of Tyr188 (N8B-O (Tyr188) = 2.8 Å) are present in complexes of both wild-type and mutant Lys103Asn RT with loviride. The overall location of loviride in the wild-type and mutant complexes are very similar, with the maximum displacements observed in the outermost portions of the dihalogenated ring system. Some of the differences between the loviride wild-type and mutant complexes may be because the wild-type structure determination used crystals cooled to −10 °C[18] and the Lys103Asn mutant complex determination used flash-frozen crystals (−165 °C). Overall, however, both HBY 097 and loviride interact similarly with Lys103Asn mutant and wild-type HIV-1 RT.

A network of hydrogen bonds in the NNIBP region of unliganded Lys103Asn mutant HIV-1 RT

The overall structure of unliganded Lys103Asn mutant HIV-1 RT is similar to unliganded wild-type RT.[28,29] In both structures, the p66 thumb subdomain is folded into the DNA-binding cleft, and the NNIBP does not exist in either structure (Figure 2). A comparison based on superposition of all C^{α} atoms gives an RMS deviation of 0.69 Å. The RMS deviation is 0.44 Å for the C^{α} atoms in the NNIBP region, indicating an overall similarity of main-chain conformation in the binding-pocket region between the mutant and wild-type RT.

Substitution of asparagine for lysine at position 103 leads to important differences in the structure of the NNIBP region between the Lys103Asn mutant and wild-type HIV-1 RT structures without bound NNRTIs (Figure 2). In the Lys103Asn mutant RT structure, the long and positively charged lysine side-chain is replaced with the relatively smaller neutral C^{γ}-branched side-chain of asparagine at position 103. The side-chain of Asn103 retains an orientation similar to that of Lys103 in the wild-type structure; the empty space left by the substitution of Asn for the Lys103 side-chain is occupied by a water molecule (Wat3). A key hydrogen bond is formed between the side-chain atom $N^{\delta 2}$ of Asn103 and the side-chain phenoxyl group (O^{η}) of Tyr188 in the unliganded Lys103Asn mutant RT ($d = 3.1$ Å; angle = 130 °), which does not exist in the wild-type HIV-1 RT structure; the observation of this hydrogen bond in the Lys103Asn mutant HIV-1 RT confirms the prediction by Ren *et al.*, which was based on molecular modeling studies of HIV-1 RT/NNRTI complexes.[25] Another hydrogen bond is observed between the side-chain atom $N^{\delta 2}$ of Asn103 and the main-chain carbonyl oxygen atom of Lys101 ($d = 3.2$ Å; angle = 123 °). The side-chain atom $O^{\delta 1}$ of Asn103 forms a hydrogen bond with Wat3 ($d = 3.2$ Å; angle = 117 °). A water molecule (Wat2; see Figure 3) is conserved in both the unliganded wild-type and Lys103Asn mutant HIV-1 RT structures. Wat2 forms a hydrogen bond with the main-chain carbonyl oxygen atom of Lys101 ($d = 3.1$ Å) and a weak hydrogen bond with the side-chain phenoxyl group (O^{η}) of Tyr188 ($d = 3.7$ Å). The orientation and position of the Tyr181 side-chain differs significantly in the Lys103Asn mutant and wild-type RT structures. Another conserved water molecule (Wat1) in the NNIBP region forms only a weak hydrogen bond with the amide group of Lys101 ($d = 3.8$ Å; angle = 116 °) in the unliganded wild-type HIV-1 RT structure. In the Lys103Asn mutant RT structure, Wat1 also forms a hydrogen bond with the side-chain phenoxyl group (O^{η}) of

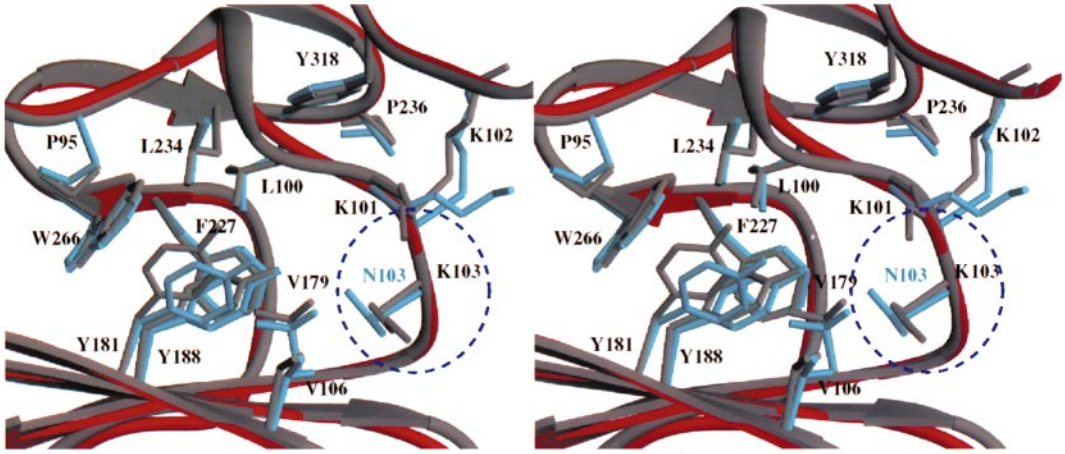

Figure 2. Stereoview of a superposition of unliganded wild-type and Lys103Asn mutant HIV-1 RT in the NNIBP region. Wild-type HIV-1 RT is shown in gray, mutant HIV-1 RT in red ribbon with cyan side-chains. The blue circle highlights the position of residue 103.

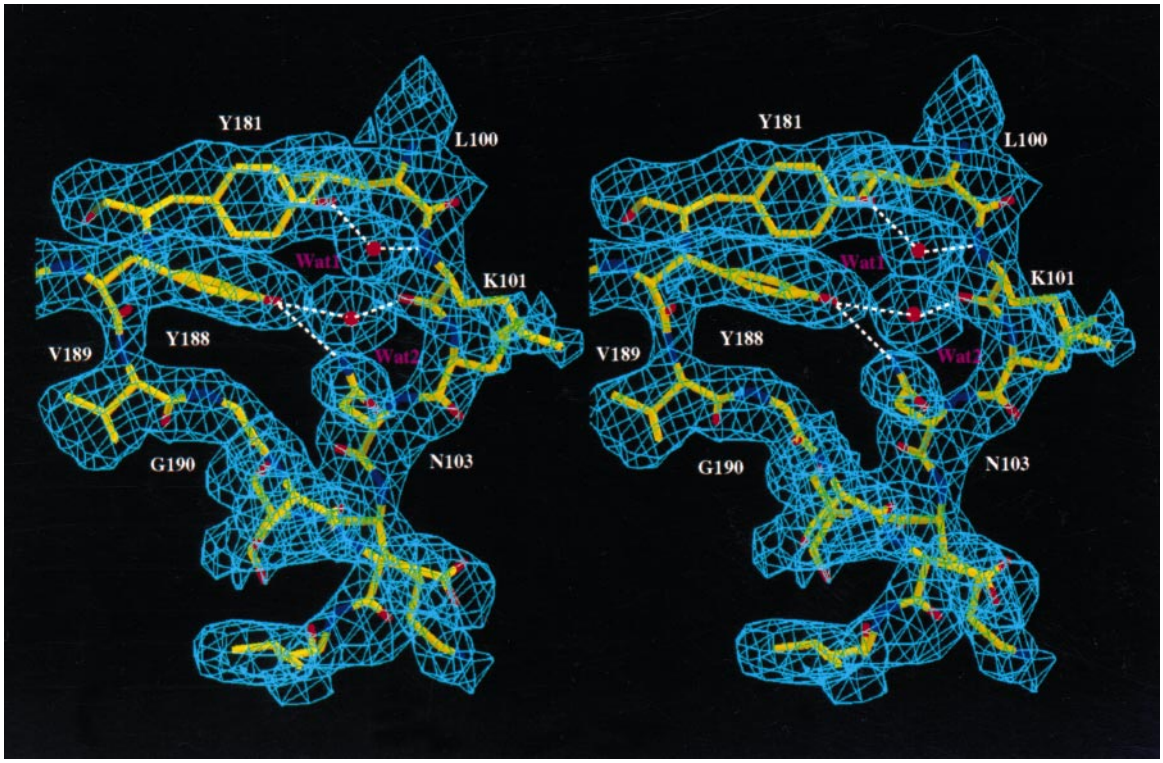

Figure 3. Stereoview of a SIGMAA weighted $2mF_o - DF_c$ difference Fourier map showing the electron density in the NNIBP region of p66 in the unliganded Lys103Asn mutant HIV-1 RT structure. The phases were computed from the final model at 2.7 Å resolution and the map was contoured at 2σ. Selected hydrogen-bonding interactions are indicated with broken lines.

Tyr181 ($d = 3.1$ Å; angle = 117°) in addition to the hydrogen bond with the amide nitrogen atom of Lys101 ($d = 2.8$ Å; angle = 112°), effectively displacing the side-chain phenoxyl group of Tyr181 toward Wat2 by 2.0 Å. In addition, the side-chain of Lys101 has also changed position (Figure 2). These changes may be due, in part, to the difference in the total charge in this region that results from replacing lysine with asparagine. Conceivably, this network of hydrogen bonds would stabilize the structure of the NNIBP region (and the closed-pocket form of the enzyme) in the Lys103Asn mutant RT.

In both the wild-type and Lys103Asn mutant HIV-1 RT structures, no conserved water molecules exist in the corresponding region of p51. In wild-type HIV-1 RT, the side-chain atom N^{ζ} of Lys103 of p51 forms a hydrogen bond with the carbonyl oxygen atom of Asp172 of p51 ($d = 3.2$ Å; angle = 122°) and a salt-bridge with the side-chain $O^{\delta 2}$ atom of Asp192 of p51 ($d = 3.3$ Å; angle = 111°). In the p51 subunit of Lys103Asn mutant HIV-1 RT, the side-chain $N^{\delta 2}$ atom of Asn103 forms hydrogen bonds with the main-chain carbonyl oxygen atoms of Gly99 ($d = 2.9$ Å; angle = 152°) and Leu100 ($d = 2.9$ Å; angle = 126°). However, the p51 subunit does not contain an NNIBP and does not bind NNRTIs in the HIV RT p66/p51 heterodimer.

Novel drug-resistance mechanism: Lys103Asn mutation interferes with formation of the inhibitor-binding pocket

As asserted earlier, the inhibitor-bound mutant RT structures have conformations of the NNIBP that are similar to the wild-type RT/NNRTI structures. This suggests that protein and inhibitors make similar interactions in both the wild-type and mutant RT complexes with inhibitors. Some small changes have occurred in the position and orientation of the bound inhibitors, and these are most pronounced in the flexible side-groups of HBY 097. Such changes are reminiscent of those seen between wild-type and Tyr188Leu mutant HIV-1 RT complexes with HBY 097,[22] and may correlate with the specific variation of Lys103Asn resistance to different NNRTIs.

Small but important changes observed between the structures of the unliganded wild-type and Lys103Asn mutant HIV-1 RT in the NNIBP region may account for the broad cross-resistance of this mutant to most NNRTIs. Earlier studies indicated that residue 103 was located near a putative entrance to the NNIBP and that most NNRTIs do not make significant interactions with Lys103 in their complexes with wild-type HIV-1 RT. The present study has revealed a network of hydrogen bonds in the NNIBP region of the unliganded

Lys103Asn mutant RT that is not present in wild-type HIV-1 RT.

Given the differences between the structures of the unliganded Lys103Asn mutant and wild-type HIV-1 RT, the Lys103Asn mutant and wild-type RT must undergo different conformational changes during the process of drug binding. Differences in the binding pathway would incur different energetic costs for Lys103Asn mutant and wild-type RT, which could account for the observed drug resistance. In particular, hydrogen bonds between the Asn103 and Tyr188 side-chains and the Tyr181 side-chain and a water molecule (Wat2; Figure 3) present in the Lys103Asn mutant but not in wild-type HIV-1 RT may stabilize the closed form of the NNIBP. These hydrogen bonds must be broken during the drug-binding process, incurring an additional energetic cost in forming the pocket and thereby interfering with inhibitor entry. The side-chains of Tyr181 and Tyr188 reorient during the formation of the NNIBP during the process of NNRTI binding, effectively ''flipping'' toward the polymerase active site.[15]

An interpretation consistent with the available data would be that the unbound state of Lys103Asn mutant is more stable than that of wild-type HIV-1 RT relative to their respective NNRTI-bound complexes, which are expected to have similar free energies (Figure 4). In this mechanistic model, the Lys103Asn mutation stabilizes the unbound state of HIV-1 RT relative to wild-type more than it affects the inhibitor-bound form of RT. This is a different resistance mechanism from those found for the Tyr181Cys mutant[16] or the Tyr188Leu mutant,[22] both of which involve loss of interactions between the protein and the bound inhibitor.

The proposed drug-resistance mechanism represented schematically in Figure 4 implies that HIV-1 RT containing the Lys103Asn mutation would have a slower rate of drug binding (lower on rate), but a similar rate of dissociation of the NNRTI (similar off rate). A kinetic analysis showed that the Lys103Asn mutation reduced the on rate for nevirapine, but did not affect the rate of dissociation,[33] consistent with this model. In this novel drug-resistance mechanism, Asn103 of the Lys103Asn mutant HIV-1 RT acts as a gatekeeper, controlling the entrance of the drug to the NNIBP.

Implications for drug design

We have presented a new mechanism for drug resistance that could explain the reduced susceptibility of Lys103Asn mutant HIV-1 RT to NNRTIs. The mutation leads to a stabilization of the closed-pocket form of the enzyme, which could result in decreased rate of drug binding to RT. This would explain the broad spectrum of cross-resistance to NNRTIs associated with this mutation and the selection of Lys103Asn by many structurally unrelated NNRTIs in the clinical setting.

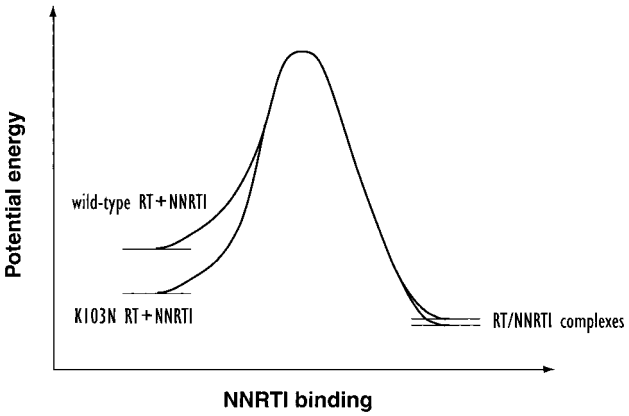

Figure 4. Energy diagram for the binding of an NNRTI to wild-type and Lys103Asn mutant RT. The Lys103Asn mutant RT with the additional hydrogen bonding network in the NNIBP region is assumed to be more stable than wild-type HIV-1 RT. The relative stability of wild-type and Lys103Asn mutant HIV-1 RT complexes with NNRTIs will depend on the inhibitor.

However, it is possible that some NNRTIs that are relatively potent in inhibiting Lys103Asn HIV-1 RT have stabilizing interactions with Asn103 in the drug-bound mutant complex that are not present with Lys103 in the respective complex with wild-type HIV-1 RT. Likewise, NNRTIs that are particularly ineffective against Lys103Asn HIV-1 RT may, in some cases, lose stabilizing interactions with Lys103 when Lys103 is replaced with Asn. The observed range of Lys103Asn resistance to different NNRTIs may be due, in part, to subtle variations in Lys103 or Asn103 interactions with the bound NNRTI. These considerations suggest that NNRTIs that can make favorable interactions with Asn103 without compromising inhibitory activity against wild-type HIV-1 RT could encounter less drug resistance with the Lys103Asn mutation. The current suggestions can be combined with the previous suggestion that inhibitor flexibility could be a useful design feature for reducing drug resistance.[22]

Materials and Methods

Crystallization, data collection, and structure determination

The unliganded, loviride-bound, and HBY 097-bound Lys103Asn mutant HIV-1 RT samples used in crystallization were prepared by methods similar to those described previously.[16–18,22,28,34] The NNRTIs loviride and HBY 097 were co-crystallized with Lys103Asn mutant HIV-1 RT in hanging-drop vapor diffusion set-ups. NNRTI-containing solution (20 mM NNRTI in dimethylsulfoxide (DMSO) and 5% (w/v) *n*-octyl β-D-glucopyranoside (β-OG)) was mixed with thawed HIV-1 RT concentrate (30 mg ml^{-1} in 10 mM Tris-HCl (pH 8.0) and 75 mM NaCl) in a 2:1 inhibitor:RT molar ratio. The hanging drops were prepared by adding equal volumes

Table 1. Summary of crystallographic data and refinement statistics

	Unliganded Lys103Asn HIV-1 RT	Lys103Asn HIV-1 RT/HBY 097 complex	Lys103Asn HIV-1 RT/loviride complex
PDB entry code	1HQE	1HQU	1HPZ
Radiation source	CHESS (F1)	CHESS (F1)	CHESS (F1)
No. of crystals	1	2	1
No. of images	111	136	102
Temperature (°C)	−165°	−165°	−165°
Resolution range (Å)	50-2.7	50-2.8	50-3.0
Cell parameters			
a (Å)	236.1	223.9	223.1
b (Å)	70.4	68.9	69.0
c (Å)	93.4	103.9	104.0
β (deg.)	106.2	106.4	106.8
No. of unique reflections	37,652	35,562	29,927
Completeness (%)	92.2 (87.6)	94.4 (52.7)	97.7 (94.2)
R_{merge} (%)[a]	10.1 (37.6)	15.3 (46.8)	13.5 (37.0)
		Refinement statistics	
Resolution range (Å)	25-2.7	25-2.8	25-3.0
No. of reflections	36,086	34,254	28,432
Completeness (%)	88.4 (73.0)	90.9 (43.9)	92.8 (78.8)
R-factor[b] (%)	25.0 (35.9)	24.9 (34.1)	25.9 (34.5)
Free *R*-factor (%)	33.1 (38.5)	34.5 (39.9)	34.4 (35.6)
No. of protein atoms	7657	7799	7799
No. of water molecules	182	0	0
Average *B*-factor (Å^2)	64.8	61.8	63.9
Luzzati error (Å)	0.42 (0.56)	0.42 (0.58)	0.44 (0.57)
RMS deviations			
Bond (Å)	0.01	0.01	0.01
Angles (deg.)	1.7	1.7	0.9

The corresponding statistics for the highest resolution shell are listed in parentheses. The highest resolution shell for the unliganded Lys103Asn HIV-1 RT is 2.7-2.8 Å, for the Lys103Asn HIV-1 RT/HBY 097 complex, 2.8-2.9 Å, and for the Lys103Asn HIV-1 RT/loviride complex, 3.0-3.1 Å, respectively.

[a] $R_{merge} = \Sigma|I_{obs} - \langle I\rangle|/\Sigma\langle I\rangle$.

[b] $R = \Sigma||F_{obs}| - |F_{cal}||/\Sigma|F_{obs}|$.

of the protein/inhibitor and crystallization solutions (50 mM bis-Tris-propane, 100 mM $(NH_4)_2SO_4$, 10% (w/v) glycerol, and 9% (w/v) PEG 8000, pH 6.8). Crystals were obtained by microseeding with crushed unliganded wild-type HIV-1 RT crystals.[28] Crystals used for data collection grew to an average size of 0.1 mm × 0.3 mm × 0.7 mm, approximately four days after seeding.

Diffraction datasets for the unliganded and inhibitor-bound mutant HIV-1 RT complex were collected at the Cornell High Energy Synchrotron Source (CHESS) F1 beam line ($\lambda = 0.91$ Å) at −165°C and recorded on a 2 K × 2 K CCD detector in the binned mode. Reflections were indexed and intensities were integrated using DENZO and scaled and postrefined using SCALEPACK in the HKL package;[35,36] intensities of partial reflections on abutting frames were added. Both the unliganded and NNRTI-bound Lys103Asn mutant crystals had the symmetry of space group *C*2 with cell parameters comparable to those of their respective wild-type crystal forms.[18,22,28] The diffraction data statistics are summarized in Table 1.

All three structures were solved by the molecular replacement method using the corresponding wild-type RT coordinates with alanine at residue 103 as the starting models. The starting models used for solving the NNRTI-bound Lys103Asn HIV-1 RT complexes did not contain coordinates for the NNRTIs. Rounds of model building were guided using both SIGMAA weighted difference Fourier ($2mF_o - DF_c$) and omit maps. The position and orientation of bound inhibitors were interpreted using SIGMAA weighted difference Fourier ($mF_o - DF_c$) maps prior to inclusion of inhibitors in the phasing model. Structure refinement was performed using both conventional and torsion-constrained refinement protocols in X-PLOR.[37,38] Refinement statistics are listed in Table 1. A region of the SIGMAA weighted difference Fourier ($2mF_o - DF_c$) electron density in the NNIBP region of the unliganded Lys103Asn mutant HIV-1 RT structure is shown in Figure 3.

Protein Data Bank accession numbers

Coordinates for the unliganded Lys103Asn mutant HIV-1 RT, and HBY 097 and loviride complexes with Lys103Asn mutant HIV-1 RT have been deposited with the Protein Data Bank for immediate release with the PDB entry codes 1HQE, 1HQU, and 1HPZ, respectively.

Acknowledgments

We thank Pat Clark, Peter Frank, and Dave Miller for the growth of recombinant expression strains and initial purification of HIV-1 RT; Stefan Sarafianos, Wanyi Zhang, Boxu Yan, Pat Achord, and CHESS staff members for their help with X-ray data collection; Ann Stock for critical reading of the manuscript, Susan Mazzocchi for comments, and Barbara Shaver for technical assistance. NIH grants (AI 27690 and AI 36144), the Janssen Research Foundation, Hoechst General Pharma Research, and the Keck Foundation supported the research in E.A.'s laboratory when this work was done. S.H.H.'s

laboratory was sponsored ''in part'' by the National Cancer Institute, DHHS, under contract with ABL and by NIGMS. The contents of this publication do not necessarily reflect the views or policies of the Department of Health and Human Services, nor does mention of trade names, commercial products, or organizations imply endorsement by the US Government.

References

1. Balzarini, J., Pelemans, H., Riess, G., Roesner, M., Winkler, I., De Clercq, E. & Kleim, J. P. (1998). Retention of marked sensitivity to (S)-4-isopropoxycarbonyl-6-methoxy-3-(methylthiomethyl)-3,4-dihydroquinoxaline-2-(1H)-thione (HBY 097) by an azidothymidine (AZT)-resistant human immunodeficiency virus type 1 (HIV-1) strain subcultured in the combined presence of quinoxaline HBY 097 and 2′,3′-dideoxy-3′-thiacytine (lamivudine). *Biochem. Pharmacol.* **55**, 617-625.
2. Balzarini, J., Velazquez, S., San-Felix, A., Karlsson, A., Perez-Perez, M.-J., Camarasa, M.-J. & De Clercq, E. (1993). Human immunodeficiency virus type 1-specific [2′,5′-bis-O-[*tert*-butyldimethylsilyl]-β-D-ribofuranosyl]-3′-spiro-5″-(4″-amino-1″,2″-oxathiole-2″,2″-dioxide)-purine analogues show a resistance spectrum that is different from that of the human immunodeficiency virus type-1-specific non-nucleoside analogues. *Mol. Pharmacol.* **43**, 109-114.
3. De Clercq, E. (1998). The role of non-nucleoside reverse transcriptase inhibitors (NNRTIs) in the therapy of HIV-1 infection. *Antiviral Res.* **38**, 153-179.
4. Demeter, L., Meehan, P., Morse, G., Fischl, M., Para, M., Powderly, W., Leedom, J., Holden-Wiltse, J., Greisberger, C., Wood, K., Timpone, J. J., Wathen, L., Resnick, L., Batts, D. & Reichman, R. (1998). Phase I study of atevirdine mesylate (U-87201E) monotherapy in HIV-1-infected patients. *J. Acquir. Immune Defic. Syndr. Hum. Retrovirol.* **19**, 135-144.
5. Richman, D. D. (1993). Resistance of clinical isolates of human immunodeficiency virus to antiretroviral agents. *Antimicrob. Agents Chemother.* **37**, 1207-1213.
6. Rubsamen-Waigmann, H., Huguenel, E., Shah, A., Paessens, A., Ruoff, H. J., von Briesen, H., Immelmann, A., Dietrich, U. & Wainberg, M. A. (1999). Resistance mutations selected *in vivo* under therapy with anti-HIV drug HBY 097 differ from resistance pattern selected *in vitro*. *Antivir. Res.* **42**, 15-24.
7. Staszewski, S., Miller, V., Kober, A., Colebunders, R., Vandercam, B., Delescluse, J., Clumeck, N., Van Wanzeele, F., De Brabander, M., De Cree, J., Moeremans, M., Andries, K., Bouch, C., Stoffels, P. & Janssen, P. A. J. (1996). Evaluation of the efficacy and tolence of R018893, R089439 (loviride) and placebo in asymptomatic HIV-1-infected patients. *Antivir. Ther.* **1**, 42-50.
8. Casado, J. L., Hertogs, K., Ruiz, L., Dronda, F., Cauwenberge, A. V., Arno, A., Garcia-Arata, I., Bloor, S., Bonjoch, A., Blazquez, J., Clotet, B. & Larder, B. (2000). Non-nucleoside reverse transcriptase inhibitor resistance among patients failing a nevirapine plus protease inhibitor-containing regimen. *AIDS,* **14**, F1-F7.
9. Gatell, J., Lange, J. & Gartland, M. (1999). AVANTI: randomized, double-blind trial to evaluate the efficacy and safety of zidovudine plus lamivudine versus zidovudine plus lamivudine plus loviride in HIV-infected antiretroviral-naive patients. AVANTI Study Group. *Antivir. Ther.* **4**, 79-86.
10. Hayashi, S., Jayesekera, D., Jayewardene, A., Shah, A., Thevanayagam, L. & Aweeka, F. (1999). Altered pharmacokinetics of indinavir by a novel nonnucleoside reverse transcriptase (HBY 097): a pharmacokinetic evaluation in HIV-positive patients. *J. Clin. Pharmacol.* **39**, 1085-1093.
11. Kleim, J.-P., Winters, M., Dunkler, A., Suarez, J.-R., Riess, G., Winkler, R., Balzarini, J., Oette, D., Merigan, T. C. & Group, T. H. S. (1999). Antiviral activity of the human immunodeficiency virus type 1-specific nonnucleoside reverse transcriptase inhibitor HBY 097 alone and in combination with Zidovudine in a phase II study. *J. Infect. Dis.* **179**, 709-713.
12. Miller, V., De Bethune, M. P., Kober, A., Aturmer, M., Hertogs, K., Pauwels, R., Stoffels, P. & Staszewski, S. (1998). Patterns of resistance and cross-resistance to human immunodeficiency virus type 1 reverse transcriptase inhibitors in patients treated with the nonnucleoside reverse transcriptase inhibitor loviride. *Antimicrob. Agents Chemother.* **42**, 3123-3129.
13. Huang, H., Chopra, R., Verdine, G. L. & Harrison, S. C. (1998). Structure of a covalently trapped catalytic complex of HIV-1 reverse transcriptase: implications for drug resistance. *Science,* **282**, 1669-1675.
14. Ding, J., Das, K., Hsiou, Y., Sarafianos, S. G., Clark, A. D., Jr, Jacobo-Molina, A., Tantillo, C., Hughes, S. H. & Arnold, E. (1998). Structure and functional implications of the polymerase active site region in a complex of HIV-1 RT with double-stranded DNA and an antibody Fab fragment at 2.8 Å resolution. *J. Mol. Biol.* **284**, 1095-1111.
15. Jacobo-Molina, A., Ding, J., Nanni, R. G., Clark, A. D., Jr, Lu, X., Tantillo, C., Williams, R. L., Kamer, G., Ferris, A. L., Clark, P., Hizi, A., Hughes, S. H. & Arnold, E. (1993). Crystal structure of human immunodeficiency virus type 1 reverse transcriptase complexed with double-stranded DNA at 3.0 Å resolution shows bent DNA. *Proc. Natl Acad. Sci. USA,* **90**, 6320-6324.
16. Das, K., Ding, J., Hsiou, Y., Clark, A. D., Jr, Moereels, H., Koymans, L., Andries, K., Pauwels, R., Janssen, P. A. J., Boyer, P. L., Clark, P., Smith, J. R. H., Kroeger Smith, M. B., Michejda, C. J., Hughes, S. H. & Arnold, E. (1996). Crystal structures of 8-Cl and 9-Cl TIBO complexed with wild-type HIV-1 RT and 8-Cl TIBO complexed with the Tyr181Cys HIV-1 RT drug-resistant mutant. *J. Mol. Biol.* **264**, 1085-1100.
17. Ding, J., Das, K., Moereels, H., Koymans, L., Andries, K., Janssen, P. A. J., Hughes, S. H. & Arnold, E. (1995a). Structure of HIV-1 RT/TIBO R 86183 reveals similarity in the binding of diverse nonnucleoside inhibitors. *Nature Struct. Biol.* **2**, 407-415.
18. Ding, J., Das, K., Tantillo, C., Zhang, W., Clark, A. D., Jr, Jessen, S., Lu, X., Hsiou, Y., Jacobo-Molina, A., Andries, K., Pauwels, R., Moereels, H., Koymans, L., Janssen, P. A. J., Smith, R., Koepke, M. K., Michejda, C., Hughes, S. H. & Arnold, E. (1995b). Structure of HIV-1 reverse transcriptase in a complex with the nonnucleoside inhibitor α-APA R 95845 at 2.8 Å resolution. *Structure,* **3**, 365-379.
19. Esnouf, R., Ren, J., Hopkins, A., Ross, C., Jones, E., Stammers, D. & Stuart, D. (1997). Unique features in the structure of the complex between HIV-1 reverse transcriptase and the bis(heteroaryl)piperazine

(BHAP) U-90152 explain resistance mutations for this nonnucleoside inhibitor. *Proc. Natl Acad. Sci. USA,* **94**, 3984-3989.
20. Hopkins, A. L., Ren, J., Esnouf, R. M., Willcox, B. E., Jones, E. Y., Ross, C., Miyasaka, T., Walker, R. T., Tanaka, H., Stammers, D. K. & Stuart, D. I. (1996). Complexes of HIV-1 reverse transcriptase with inhibitors of the HEPT series reveal conformational changes relevant to the design of potent non-nucleoside inhibitors. *J. Med. Chem.* **39**, 1589-1600.
21. Hopkins, A. L., Ren, J., Tanaka, H., Baba, M., Okamato, M., Stuart, D. I. & Stammers, D. K. (1999). Design of MKC-442 (emivirine) analogues with improved activity against drug-resistant HIV mutants. *J. Med. Chem.* **42**, 4500-4505.
22. Hsiou, Y., Das, K., Ding, J., Clark, J. A. D., Kleim, J.-P., Roesner, M., Winkler, I., Riess, G., Hughes, S. H. & Arnold, E. (1998). Structures of Tyr188Leu mutant and wild-type HIV-1 reverse transcriptase complexed with the non-nucleoside inhibitor HBY 097: inhibitor flexibility is a useful design feature for reducing drug resistance. *J. Mol. Biol.* **284**, 313-323.
23. Kohlstaedt, L. A., Wang, J., Friedman, J. M., Rice, P. A. & Steitz, T. A. (1992). Crystal structure at 3.5 Å resolution of HIV-1 reverse transcriptase complexed with an inhibitor. *Science,* **256**, 1783-1790.
24. Ren, J., Diprose, J., Warren, J., Esnouf, R., Bird, L. E., Ikemizu, S., Slater, M., Milton, J., Balzarini, J., Stuart, D. I. & Stammers, D. K. (2000). Phenyl ethylthiazolylthiourea (PETT) non-nucleoside inhibitors of HIV-1 and HIV-2 reverse transcriptase. *J. Biol. Chem.* **275**, 5633-5639.
25. Ren, J., Esnouf, R., Garman, E., Somers, D., Ross, C., Kirby, I., Keeling, J., Darby, G., Jones, Y., Stuart, D. & Stammers, D. (1995a). High resolution structures of HIV-1 RT from four RT-inhibitor complexes. *Nature Struct. Biol.* **2**, 293-302.
26. Ren, J., Esnouf, R., Hopkins, A., Ross, C., Jones, Y., Stammers, D. & Stuart, D. (1995b). The structure of HIV-1 reverse transcriptase complexed with 9-chloro-TIBO: lessons for inhibitor design. *Structure,* **3**, 915-926.
27. Esnouf, R., Ren, J., Ross, R., Jones, Y., Stammers, D. & Stuart, D. (1995). Mechanism of inhibition of HIV-1 reverse transcriptase by non-nucleoside inhibitors. *Nature Struct. Biol.* **2**, 303-308.
28. Hsiou, Y., Ding, J., Das, K., Clark, A. D., Jr, Hughes, S. H. & Arnold, E. (1996). Structure of unliganded HIV-1 reverse transcriptase at 2.7 Å resolution: implications of conformational changes for polymerization and inhibition mechanisms. *Structure,* **4**, 853-860.
29. Rodgers, D. W., Gamblin, S. J., Harris, B. A., Ray, S., Culp, J. S., Hellmig, B., Woolf, D. J., Debouck, C. & Harrison, S. C. (1995). The structure of unliganded reverse transcriptase from the human immunodeficiency virus type 1. *Proc. Natl Acad. Sci. USA,* **92**, 1222-1226.
30. Ren, J., Esnouf, R. M., Hopkins, A. L., Jones, E. Y., Kirby, I., Keeling, J., Ross, C. K., Larder, B. A., Stuart, D. I. & Stammers, D. K. (1998). 3′-Azido-3′-deoxythymidine drug resistance mutations in HIV-1 reverse transcriptase can induce long range conformational changes. *Proc. Natl Acad. Sci. USA,* **95**, 9518-9523.
31. Sarafianos, S. G., Das, K., Clark, A. D., Jr, Ding, J., Boyer, P. L., Hughes, S. H. & Arnold, E. (1999). Lamivudine (3TC) resistance in HIV-1 reverse transcriptase involves steric hindrance with β-branched amino acids. *Proc. Natl Acad. Sci. USA,* **96**, 10027-10032.
32. Ren, J., Milton, J., Weaver, K. L., Short, S. A., Stuart, D. I. & Stammers, D. K. (2000). Structural basis for the resilience of efavirenz (DMP-266) to drug resistance mutations in HIV-1 reverse transcriptase. *Struct. Fold. Des.* **8**, 1089-1094.
33. Maga, G., Amacker, M., Ruel, N., Hubscher, U. & Spadari, S. (1997). Resistance to nevirapine of HIV-1 reverse transcriptase mutants: loss of stabilizing interactions and thermodynamic or steric barriers are induced by different single amino acid substitutions. *J. Mol. Biol.* **274**, 738-747.
34. Clark, A. D., Jr, Jacobo-Molina, A., Clark, P., Hughes, S. H. & Arnold, E. (1995). Crystallization of human immunodeficiency virus type 1 reverse transcriptase with and without nucleic acid substrates, inhibitors and an antibody Fab fragment. *Methods Enzymol.* **262**, 171-185.
35. Gewirth, D. (1995). *The HKL manual*, HKL Research, Inc. Charlottesville, VA.
36. Otwinowski, Z. & Minor, W. (1996). Processing of X-ray diffraction data collected in oscillation mode. *Methods Enzymol.* **276**, 55-62.
37. Brunger, A. T. (1993). *X-PLOR Manual Version 3.1: A system for X-ray Crystallography and NMR*, Yale University Press, New Haven and London.
38. Rice, L. M. & Brunger, A. T. (1994). Torsion angle dynamics: reduced variable conformational sampling enhances crystallographic structure refinement. *Proteins: Struct. Funct. Genet.* **19**, 277-290.

Edited by J. Karn

(Received 26 October 2000; received in revised form 23 March 2001; accepted 23 March 2001)